8th International Congress of Croatian Society of Mechanics
29 September – 2 October 2015
Opatija, Croatia

On the Optimization of Shape Parameters in the Local Radial Point Interpolation Collocation Method for Modeling of Heterogeneous Materials

Boris JALUŠIĆ, Tomislav JARAK, Jurica SORIĆ

Faculty of Mechanical Engineering and Naval Architecture, University of Zagreb, Ivana Lučića 5, 10000 Zagreb, Croatia.
E-mails: {boris.jalusic, tomislav.jarak, jurica.soric}@fsb.hr

Abstract. A meshless Radial Point Interpolation Collocation Method (RPICM) is applied for the modeling of heterogeneous structures consisting of homogeneous materials. Two homogeneous isotropic materials with different material properties are considered. The solution for the entire heterogeneous structure is obtained by enforcing appropriate displacement continuity and traction reciprocity conditions along the interface of homogeneous subdomains. For the approximation of the unknown field variables, the Radial Point Interpolation Method with Polynomial Reproduction (RPIM) is utilized. In the RPIM Gaussian radial basis function with one dimensionless shape parameter α_c is applied. The dependance of the accuracy and numerical efficiency on the choice of shape parameter α_c is tested. Both standard fully displacement (primal) and mixed approaches in RPICM method are considered and their efficiency is demostrated on a representative numerical example.

1 Introduction

Meshless methods are a relatively new group of numerical approaches that possess enormous potential and have made significant progress in science and engineering, especially in the area of computational mechanics [1]. This type of numerical methods can overcome some problems associated with well-known mesh-based methods, like the finite element method (FEM). Hence, they eliminate such problems as element distorsion and computationally demanding mesh generation process. Further, meshless methods that employ radial basis functions (RBF) own some clear advantages in comparison to other meshless methods due to numerically simpler construction of interpolatory meshless functions [2]. Traditional radial basis function methods that use global domain approximation yield fully-populated matrices [3], which is a big limitation to their wider engineering application.

Therefore, in this contribution, efficient Radial Point Interpolation Collocation Method (RPICM) [4] is utilized, which uses RBFs in a locally supported domains, so that the obtained system of equations is sparse, which decreases required computational effort. In addition, since the collocation sheme is adopted, there is no need for numerical integration and the method is simple and straightforward to implement. RPICM formulation is investigated for the modeling of deformation responses of heterogeneous structures. A heterogeneous structure consists of two homogeneous materials which are discretized by two sets of grid points in which equilibrium equations are imposed, while a double node is concept employed along their interface. For the approximation of the

unknown field variables in each homogeneous material, the Radial Point Interpolation Method with Polynomial Reproduction (RPIM) [1] is utilized in such a way that each material is treated as a separate problem [5]. The global solution for the entire heterogeneous structure is attained by using appropriate displacement and traction conditions along the interface of two homogeneous materials. In RPIM, well-known Gaussian radial basis function [4] with only one dimensionless shape parameter α_c is employed. Since the constructed meshless approximation functions possess interpolatory conditions the displacement boundary conditions are imposed in a simple way as in FEM. Traction boundary conditions on outer edges are enforced via the direct collocation approach.

In RPICM, a standard fully displacement (primal) [6] and a mixed approach [7] are both considered for solving the linear elastic boundary value problem for each homogeneous material. Using both approaches, a final system of discretized equations with displacement components as only unknowns is obtained. In the primal approach, this is achieved simply by using only the interpolations of displacement components. In the mixed approach, both displacement and stress components interpolations are utilized simultaneously. The nodal stress values are then expressed in terms of the approximated displacement components using the kinematic and constitutive relations in order to obtain solvable system of equations in terms of nodal displacements only. It is generally known that the accuracy of the meshless collocation methods greatly depends on the parameters used in the analysis of each separate problem. Therefore, in this contribution, the dependence of the accuracy of the solution on the local support domain size and the Gaussian radial basis function shape parameter α_c for both approaches is investigated.

The considered meshless RPICM for modeling of material discontinuity is presented in detail in chapter 2. Governing equations and obtained discretized equations for each of the considered approaches are shown. Efficiency and numerical stability depending on the meshless parameters for both primal and mixed RPICM are thoroughly investigated in chapter 3 on a numerical example of heterogeneous cylinder with imposed essential boundary conditions.

2 RPICM for modeling of heterogeneous materials

A two-dimensional heterogeneous material which occupies the global computational domain Ω surrounded by the global outer boundary Γ is considered, as shown in Figure 1.

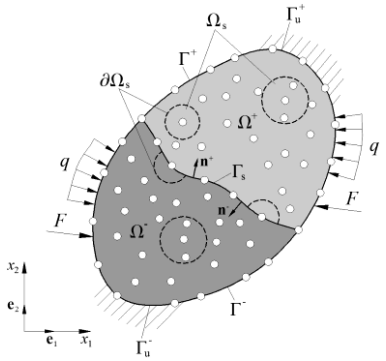

Figure1: Two-dimensional heterogeneous material

The boundary Γ_s represents the interface between two material Ω^+ i Ω^- with different properties. Γ_s separates the global domain Ω in such a manner that $\Omega = \Omega^+ \cup \Omega^-$ and $\Gamma = \Gamma^+ \cup \Gamma^-$.

The governing equations for the heterogeneous material presented in the Figure 1 are the strong form 2D equilibrium equations which have to be complied within the global computational domain Ω. The governing equations are written seperately for each material that composes the heterogeneous structure, Ω^+ and Ω^- respectively

$$\sigma^+_{ij,x_j} + b^+_i = 0, \text{ within } \Omega^+, \quad \sigma^-_{ij,x_j} + b^-_i = 0, \text{ within } \Omega^-. \tag{1}$$

Equilibrium equations (1) have to satisfy the boundary conditions prescribed on the local subdomain boundaries $\partial\Omega$

$$u^+_i = \overline{u}^+_i, \text{ on } \Gamma^+_u, \quad u^-_i = \overline{u}^-_i, \text{ on } \Gamma^-_u, \tag{2}$$

$$t^+_i = \sigma^+_{ij} n^+_j = \overline{t}^+_i, \text{ on } \Gamma^+_t, \quad t^-_i = \sigma^-_{ij} n^-_j = \overline{t}^-_i, \text{ on } \Gamma^-_t, \tag{3}$$

and the displacement continuity and traction reciprocity conditions on the interface boundary Γ_s. Since the double node concept is utilized for the dicretization of interface boundary, at each node on Γ_s relations

$$u^+_i - u^-_i = 0, \quad t^+_i + t^-_i = 0, \tag{4}$$

have to be fulfilled. The external boundary of the local subdomain $\partial\Omega$ is in general divided into two parts $\partial\Omega = \Gamma_u \cup \Gamma_t$, where $\Gamma_u = \Gamma^+_u \cup \Gamma^-_u$ represents the part of $\partial\Omega$ where the boundary displacements $\overline{u}_i$ are prescribed, while $\Gamma_t = \Gamma^+_t \cup \Gamma^-_t$ denotes the part of $\partial\Omega$ where the boundary tractions $\overline{t}_i$ are enforced.

The two-dimensional heterogeneous structure is discretized by two different sets of nodes $I = 1, 2, ..., N$ and $M = 1, 2, ..., P$ where N and P indicate the total number of nodes within materials Ω^+ and Ω^-, respectively. In the fully displacement (primal) approach, the only unknown field variables are the displacement components, while in the mixed approach both the displacement and stress components are considered as the unknown field variables. In both approaches, the unknown field variables are approximated separately within materials Ω^+ and Ω^-. In the mixed approach, same approximation functions are utilized for all the displacement and stress components. Therefore, for the material Ω^-, the displacement approximation function

$$u^{-(h)}_i(\mathbf{x}) = \sum_{J=1}^{N_{\Omega_s}} \phi_J(\mathbf{x}) \left(\hat{u}^-_i\right)_J, \tag{5}$$

and the stress approximation function

$$\sigma^{-(h)}_{ij}(\mathbf{x}) = \sum_{J=1}^{N_{\Omega_s}} \phi_J(\mathbf{x}) \left(\hat{\sigma}^-_{ij}\right)_J, \tag{6}$$

can be written. In equations (5) and (6), ϕ_J denotes the nodal value of the two-dimensional shape function for the node J, N_{Ω_s} represents the number of nodes within the approximation domain Ω_s, while $\left(\hat{u}_i^-\right)_J$ and $\left(\hat{\sigma}_{ij}^-\right)_J$ stand for the nodal values of displacement and stress components. The same approximation functions are employed over the material Ω^+.

In order to construct shape functions needed for the calculation, the Radial Point Interpolation Method with Polynomial Reproduction (RPIM) is employed. By using N_{Ω_s} nodes in the local support domain RPIM with polynomial basis functions approximates a field variable in the form

$$f^{(h)}(\mathbf{x}) = \sum_{J=1}^{N_{\Omega_s}} R_J(\mathbf{x}) a_J + \sum_{H=1}^{m} p_H(\mathbf{x}) b_H, \tag{7}$$

where $R_J(\mathbf{x})$ is the radial basis function (RBF), $p_H(\mathbf{x})$ is polynomial basis, m is the number of polynomial basis functions, a_J and b_H are interpolation coefficients. The number of radial basis functions is determined by the number of nodes within each local support domain, while the number of polynomial basis m can be chosen based on the function reproduction requirement. The coefficients a_J and b_H are determined by enforcing that the interpolation passes through all N_{Ω_s} nodes within the support domain. After the calculation of the unknown coefficents, the final interpolation equation contains RPIM shape function defined as

$$\phi_J(\mathbf{x}) = \sum_{J=1}^{N_{\Omega_s}} R_J(\mathbf{x}) S_{Jk}^a + \sum_{H=1}^{m} p_H(\mathbf{x}) S_{Hk}^b, \tag{8}$$

where S_{Jk}^a and S_{Hk}^b stand for the elements of matrices $\mathbf{S}^a$ and $\mathbf{S}^b$, which are constant matrices for the given locations of N_{Ω_s} nodes within the support domain. More detailed derivation of RPIM shape functions in presented form can be found in [1]. There is a large number of RBF that can be used in approximation (7), such as Gaussian function, Multi-quadrics (MQ) function and Thin Plate Spline function (TPS). The classification and characteristics of the most commonly used RBFs can be found in [8]. Depending on the chosen RBF for the approximation, several shape parameters usually need to be determined. In general, these parameters are usually obtained by numerical examinations. In this contribution, the following Gaussian RBF is used

$$R_J(\mathbf{x}) = \exp\left[-\alpha_c \left(\frac{r_J}{d_c}\right)^2\right], \tag{9}$$

where $\alpha_c = c d_c$ is the dimensionless shape parameter chosen. d_c is an average nodal spacing for all nodes in the local domain of approximation. There is only one shape parameter that needs to be determined in the Gaussian radial basis function. Detailed investigation of this parameter is done for the examined numerical example in chapter 3.

2.1 Discretized equations of the fully displacement (primal) approach

In primal solution strategy, the stress components in equilibrium equations (1) are firstly rewritten using constitutive equations and kinematic relations, leading to

$$\mathbf{D}_K^{\mathrm{T}}\mathbf{D}^{+}\mathbf{D}_K\mathbf{u}^{+}\left(\mathbf{x}_I\right)+\mathbf{b}^{+}\left(\mathbf{x}_I\right)=\mathbf{0}, \qquad \mathbf{D}_K^{\mathrm{T}}\mathbf{D}^{-}\mathbf{D}_K\mathbf{u}^{-}\left(\mathbf{x}_M\right)+\mathbf{b}^{-}\left(\mathbf{x}_M\right)=\mathbf{0}, \tag{10}$$

where $\mathbf{D}_K$ denotes 2D kinematic differential operator consisting of first-order derivatives with respect to Cartesian coordinates, while $\mathbf{D}^{+}$ and $\mathbf{D}^{-}$ represent material tensors for each homogeneous material. If equations (10) are discretized by the displacement approximation (5) we obtain

$$\mathbf{D}_K^{\mathrm{T}}\mathbf{D}^{+}\sum_{J=1}^{N_{\Omega_\mathrm{s}}}\mathbf{B}_{IJ}^{+}\hat{\mathbf{u}}_J^{+}+\mathbf{b}_I^{+}=\mathbf{0}, \qquad \mathbf{D}_K^{\mathrm{T}}\mathbf{D}^{-}\sum_{J=1}^{N_{\Omega_\mathrm{s}}}\mathbf{B}_{MJ}^{-}\hat{\mathbf{u}}_J^{-}+\mathbf{b}_M^{-}=\mathbf{0}, \tag{11}$$

where $\mathbf{B}_{IJ}^{+}=\mathbf{B}_J^{+}\left(\mathbf{x}_I\right)$ and $\mathbf{B}_{MJ}^{-}=\mathbf{B}_J^{-}\left(\mathbf{x}_M\right)$ indicate the matrices consisting of the first-order derivatives of shape functions. Relations (11) represent linear algebraic equations with nodal displacements as unknowns, which can be simply rewritten as

$$\mathbf{K}_{IJ}^{+}\hat{\mathbf{u}}_J^{+}=\mathbf{R}_I^{+}, \ \text{within } \Omega^{+}, \qquad \mathbf{K}_{MJ}^{-}\hat{\mathbf{u}}_J^{-}=\mathbf{R}_M^{-}, \ \text{within } \Omega^{-}, \tag{12}$$

where nodal stiffness matrices $\mathbf{K}_{IJ}^{+}$ and $\mathbf{K}_{MJ}^{-}$ are expressed as

$$\mathbf{K}_{IJ}^{+}=\mathbf{D}_K^{\mathrm{T}}\mathbf{D}^{+}\sum_{J=1}^{N_{\Omega_\mathrm{s}}}\mathbf{B}_{IJ}^{+}, \qquad \mathbf{K}_{MJ}^{-}=\mathbf{D}_K^{\mathrm{T}}\mathbf{D}^{-}\sum_{J=1}^{N_{\Omega_\mathrm{s}}}\mathbf{B}_{MJ}^{-}, \tag{13}$$

while the nodal force vectors $\mathbf{R}_I^{+}$ and $\mathbf{R}_M^{-}$ are

$$\mathbf{R}_I^{+}=-\mathbf{b}_I^{+}, \qquad \mathbf{R}_M^{-}=-\mathbf{b}_M^{-}. \tag{14}$$

From (13) it can be easily seen that in order to assemble nodal stiffness matrices, the second-order derivatives of shape functions must be calculated. All approximation functions in this contribution possess the interpolation property at the nodes. Consequently, the displacement boundary conditions are enforced straightforward, analogously to the procedure in FEM. Therefore, by discretizing the displacement boundary conditions (2) with the approximation (5), we obtain

$$\bar{\mathbf{u}}_I^{+}=\sum_{J=1}^{N_{\Omega_\mathrm{s}}}\phi_J\hat{\mathbf{u}}_J^{+}, \ \text{ on } \Gamma_{\mathrm{u}}^{+}, \qquad \bar{\mathbf{u}}_M^{-}=\sum_{J=1}^{N_{\Omega_\mathrm{s}}}\phi_J\hat{\mathbf{u}}_J^{-}, \ \text{ on } \Gamma_{\mathrm{u}}^{-}. \tag{15}$$

Rewriting the traction boundary conditions (3) using constitutive equations and kinematic relations, and then employing displacement approximation (5) we attain

$$\bar{\mathbf{t}}_I^{+}=\mathbf{N}_I^{+}\mathbf{D}^{+}\sum_{J=1}^{N_{\Omega_\mathrm{s}}}\mathbf{B}_{IJ}^{+}\hat{\mathbf{u}}_J^{+}, \ \text{ on } \Gamma_{\mathrm{t}}^{+}, \qquad \bar{\mathbf{t}}_M^{-}=\mathbf{N}_M^{-}\mathbf{D}^{-}\sum_{J=1}^{N_{\Omega_\mathrm{s}}}\mathbf{B}_{MJ}^{-}\hat{\mathbf{u}}_J^{-}, \ \text{ on } \Gamma_{\mathrm{t}}^{-}, \tag{16}$$

where $\mathbf{N}_I^{+}=\mathbf{N}^{+}\left(\mathbf{x}_I\right)$ and $\mathbf{N}_M^{-}=\mathbf{N}^{-}\left(\mathbf{x}_M\right)$ denote matrices comprising of unit normal vector components with respect to Cartesian coordinate system. In a

similar way, the applied interface boundary conditions (4) are discretized using only the displacement approximation (5) leading to

$$\sum_{J=1}^{N_{\Omega_s}} \phi_J \hat{\mathbf{u}}_J^+ = \sum_{J=1}^{N_{\Omega_s}} \phi_J \hat{\mathbf{u}}_J^-, \quad \text{on } \Gamma_s, \tag{17}$$

$$\mathbf{N}_I^+ \mathbf{D}^+ \sum_{J=1}^{N_{\Omega_s}} \mathbf{B}_{IJ}^+ \hat{\mathbf{u}}_J^+ = -\mathbf{N}_M^- \mathbf{D}^- \sum_{J=1}^{N_{\Omega_s}} \mathbf{B}_{MJ}^- \hat{\mathbf{u}}_J^-, \quad \text{on } \Gamma_s. \tag{18}$$

2.2 Discretized equations of the mixed approach

Applying the mixed strategy, the equilibrium equations (1) are discretized by the stress approximation (6), leading to

$$\sum_{J=1}^{N_{\Omega_s}} \mathbf{B}_{IJ}^{+\mathrm{T}} \hat{\boldsymbol{\sigma}}_J^+ + \mathbf{b}_I^+ = \mathbf{0}, \ \text{within } \Omega^+, \qquad \sum_{J=1}^{N_{\Omega_s}} \mathbf{B}_{MJ}^{-\mathrm{T}} \hat{\boldsymbol{\sigma}}_J^- + \mathbf{b}_M^- = \mathbf{0}, \ \text{within } \Omega^-. \tag{19}$$

It can be verified that the number of equations at the global level obtained by (19) is less than the total number of stress unknowns. Therefore, in order to obtain the closed system of equations, the compatibility between the approximated stresses and displacements is utilized at collocation nodes

$$\hat{\boldsymbol{\sigma}}_J^+ = \mathbf{D}^+ \sum_{K=1}^{N_{\Omega_s}} \mathbf{B}_{JK}^+ \hat{\mathbf{u}}_K, \qquad \hat{\boldsymbol{\sigma}}_J^- = \mathbf{D}^- \sum_{K=1}^{N_{\Omega_s}} \mathbf{B}_{JK}^- \hat{\mathbf{u}}_K. \tag{20}$$

Inserting the discretized constitutive relations (20) into the discretized equilibrium equations (19), a solvable system of linear algebraic equations similar to (12) with only the nodal displacements as unknowns is attained. In the mixed approach, the nodal stiffness matrices $\mathbf{K}_{IJ}^+$ and $\mathbf{K}_{MJ}^-$ are defined as

$$\mathbf{K}_{IJ}^+ = \sum_{K=1}^{N_{\Omega_s}} \mathbf{B}_{KI}^{+\mathrm{T}} \mathbf{D}^+ \mathbf{B}_{JK}^+, \qquad \mathbf{K}_{MJ}^- = \sum_{K=1}^{N_{\Omega_s}} \mathbf{B}_{KM}^{-\mathrm{T}} \mathbf{D}^- \mathbf{B}_{JK}^-, \tag{21}$$

while the nodal force vectors $\mathbf{R}_I^+$ and $\mathbf{R}_M^-$ are defined according to relation (14). As can be seen from equations (21), only the first-order derivatives of shape functions must be computed to assemble the nodal stiffness matrices. The displacement boundary conditions are enforced in the same way as in the primal approach, so equations (15) hold also for the mixed approach. Applying the stress approximation (6) and the compatibility between the approximated stresses and displacements (20) in the boundary equations (3), the discretized traction boundary conditions are derived as

$$\bar{\mathbf{t}}_I^+ = \mathbf{N}_I^+ \mathbf{D}^+ \sum_{K=1}^{N_{\Omega_s}} \mathbf{B}_{IK}^+ \hat{\mathbf{u}}_K^+, \quad \text{on } \Gamma_t^+, \qquad \bar{\mathbf{t}}_M^- = \mathbf{N}_M^- \mathbf{D}^- \sum_{K=1}^{N_{\Omega_s}} \mathbf{B}_{MK}^- \hat{\mathbf{u}}_K^-, \quad \text{on } \Gamma_t^-. \tag{22}$$

The discretized interface displacement boundary conditions are the same as in primal approach (17), while the discretized traction reprocity conditions are equal to

$$\mathbf{N}_I^+\mathbf{D}^+\sum_{K=1}^{N_{\Omega_s}}\mathbf{B}_{IK}^+\hat{\mathbf{u}}_K^+ = -\mathbf{N}_M^-\mathbf{D}^-\sum_{K=1}^{N_{\Omega_s}}\mathbf{B}_{MK}^-\hat{\mathbf{u}}_K^-, \quad \text{on } \Gamma_s. \tag{23}$$

3 Numerical example

3.1 Hollow cylinder

A hollow cylinder under essential boundary conditions as shown in Figure 2 is considered. Due to the symmetry, only a quarter model is used for obtaining the meshless solutions. The geometry of the heterogeneous cylinder is defined by the inner radius $R_1 = 1$, the interface radius $R_2 = 2$ and the outer radius $R_3 = 4$. For the analysis of deformation, only structured discretizations as in Figure 2 are used. The material properties of the inner part of cylinder are $E^+ = 1$, $\nu^+ = 0.25$, while the material properties of the outer part are $E^- = 10$, $\nu^- = 0.3$.

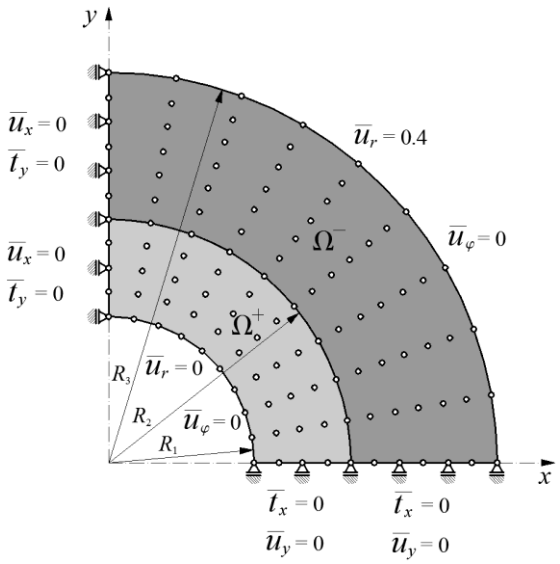

Figure2: Hollow cylinder with boundary conditions

To show the performance of the approaches presented in chapter 2 in a more clear way, the influence of the local support domain size (r_s / h_s) and the Gaussian radial basis shape parameter α_c on the accuracy of the solution is investigated. Here, the nodal distance of the uniform grid is denoted as h_s, while the circular size of the support domain is r_s, respectively. Both primal (P) and mixed (M) approaches are utilized and the obtained numerical solutions are compared with the available analytical solution [9] employing the standard relative error of displacements (e_u) in the L_2 norm [10]. For the analysis of deformation the meshless interpolation schemes using the first- and second-order basis (RPIM1, RPIM2) are applied and compared. Figures 3 through 6 show the influence of the meshless parameters on the accuracy of the obtained numerical

solutions. For the purpose of this parametric studies, the same grid of 364 nodes is employed.

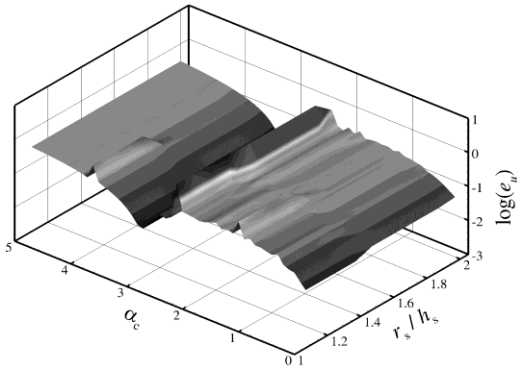

Figure3: Parametric study - 364 nodes
RPIM1 - primal approach

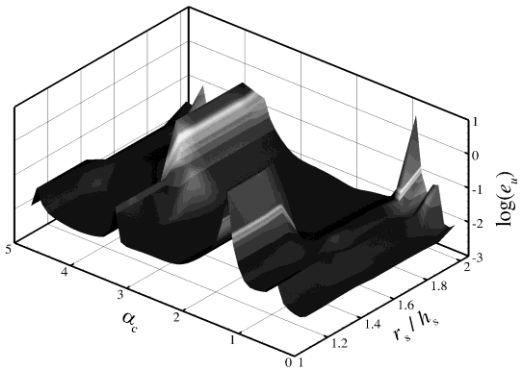

Figure4: Parametric study - 364 nodes
RPIM1 - mixed approach

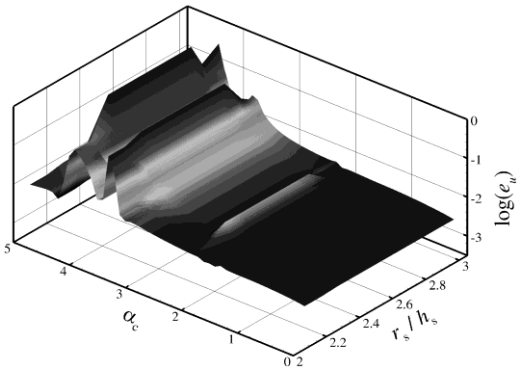

Figure5: Parametric study - 364 nodes
RPIM2 - primal approach

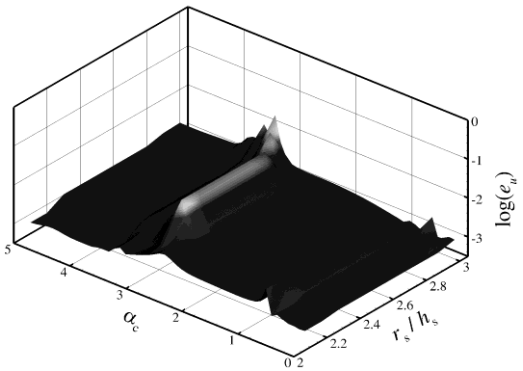

Figure6: Parametric study - 364 nodes
RPIM2 - mixed approach

As evident from the above studies, the mixed approach is superior to the primal formulation. Therefore, a more accurate and numerically stable modeling of heterogeneous materials is achieved when the mixed collocation formulation is utilized. For further verification of the presented approaches, the convergence studies of both formulations employing the relative errors e_u and e_σ in the L_2 norm of displacements and stress components are shown in Figures 7 and 8. For the purpose of creating convergence tests, some meshless parameters from the parametric studies need to be chosen. Hence, for the interpolation scheme with the first-order basis (RPIM1), the local support domain size $r_s / h_s = 1.6$ is utilized and for the scheme using the second-order basis (RPIM2) $r_s / h_s = 2.6$ is applied. In that way the same local support domain sizes are utilized for both approaches. For each of the approaches and for each order of the meshless interpolation functions, a different dimensionless radial basis shape parameter α_c is considered. Consequently, for the primal meshless formulation using the first-order basis (RPIM1-P) $\alpha_c = 3.2$ is chosen and for the mixed approach using the first-order basis (RPIM1-M) the shape parameter $\alpha_c = 2.0$ is considered. In addition, for the

primal approach with second order meshless interpolation functions (RPIM2-P) $\alpha_c = 0.5$ is applied and for the mixed formulation with second order functions (RPIM2-M) $\alpha_c = 1.5$ is utilized. From the displacement and stress convergence tests presented in Figures 7 and 8 it can be seen that better accuracy of the solution for the same number of discretization nodes is achieved when the mixed RPICM is used.

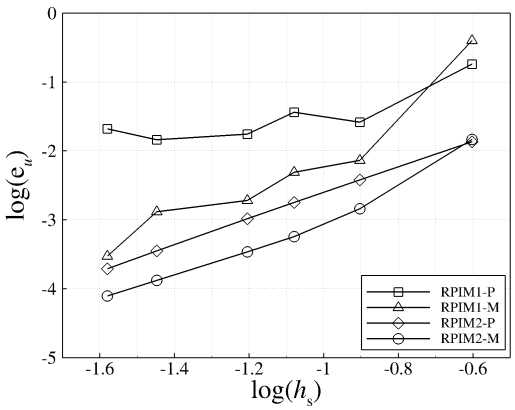

Figure7: Displacement e_u convergence test

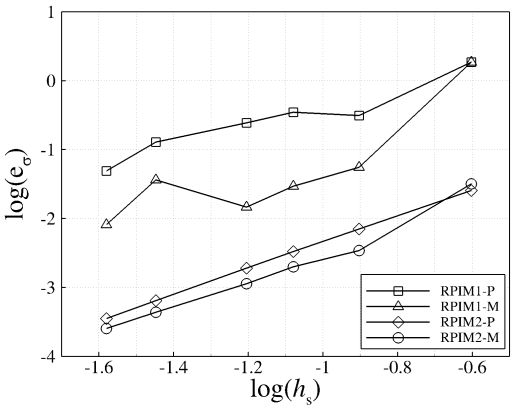

Figure8: Displacement e_σ convergence test

4 Conclusion

Two different meshless formulations of the RPICM have beed applied for the modeling of heterogeneous structures. Their efficiency has been compared by the appropriate numerical tests, and the obtained results imply the superiority of the mixed RPICM formulation. The mixed approach is more robust and less sensitive to the selection of meshless parameters, especially dimensionless shape parameters of the radial basis functions, as can be perceived from the parametric studies. Furthermore, for the same number of discretization nodes, the mixed approach results in more accurate numerical solutions. The mixed approach reduces the needed continuity order of the meshless approximation function to only C^1 continuity, while in the primal formulations C^2 continuity is needed, which increases stability and accuracy of the method. Also, the mixed RPICM method becomes more indiferent to the choice of the meshless analysis parameters as the order of the approximation function increases.

Acknowledgement
This work has been fully supported by Croatian Science Foundation under the project Multiscale Numerical Modeling of Material Deformation Responses from Macro- to Nanolevel (2516).

References

[1] Liu, G.R. Mesh Free Methods - Moving Beyond the Finite Element Method. CRC Press, 2003.

[2] Liu, G.R. Wang, J.G. A point interpolation meshless method based on radial basis functions. *International Journal for Numerical Methods in Engineering,* **54**: 1623-1648, 2002.

[3] Wang, J.G. Liu, G.R. Lin, P. Numerical analysis of Biot's consolidation process by radial point interpolation method. *International Journal of Solids and Structures,* **39**: 1557-1573, 2002.

[4] Liu, X. Liu, G.R. Tai, K. Lam, K. Y. Radial Point Interpolation Collocation Method (RPICM) for Partial Differential Equations. *Computers and Mathematics with Applications,* **50**: 1425-1442, 2005.

[5] Chen, J.-S. Wang, L. Hu, H.-Y. Chi, S.-W. Subdomain radial basis collocation method for heterogeneous media. *International Journal for Numerical Methods in Engineering,* **80**: 163-190, 2009.

[6] Atluri, S.N. Shen, S. The Meshless Local Petrov Galerkin (MLPG) Method: A Simple & Less-costly Alternative to the Finite Element and Boundary Element Methods. *CMES – Computer Modeling in Engineering & Sciences*, **3**(1): 11-51, 2002.

[7] Sorić, J. Jarak, T. Mixed meshless formulation for analysis of shell-like structures. *Computer Methods in Applied Mechanics and Engineering,* **199**: 1153-1164, 2010.

[8] Franke, C. Schaback, R. Solving partial differential equations by collocation using radial basis functions. *Applied Mathematics and Computation,* **93**: 73-82, 1997.

[9] Wang, D. Sun, Y. Li, L. A Discontinuous Galerkin Meshfree Modeling of Material Interface. *CMES – Computer Modeling in Engineering & Sciences*, **45**(1): 57-82, 2009.

[10] Jalušić, B. Sorić, J. Jarak, T. Mixed Meshless Local Petrov Galerkin (MLPG) Colocation Method for Modeling of Heterogeneous Materials. In: Onate, E. Oliver, X. Huerta A., eds., *Proceedings of the 11th World Congress on Computational Mechanics (WCCM XI)*, Barcelona, Spain, 2014.